Progress In Electromagnetics Research Letters, Vol. 91, 153–161, 2020

A Compact Dual-Band and Dual-polarized Antenna Integrated into Textile for WBAN Dual-Mode Applications

Leitao Zhou, Shaojun Fang*, and Xiao Jia

Abstract—In this letter, a compact dual-band and dual-polarized antenna integrated into textile for wireless body area network (WBAN) dual-mode applications is proposed. For on-body communication, a vertically-polarized omnidirectional radiation pattern is generated at the 2.45-GHz band. For off-body communication, a circularly polarized (CP) broadside radiation pattern is generated at the 5.8-GHz band. Both bands are realized on the same patch by loading slots and pins, which brings a compact, simple structure. Another advantage is that the textile of a full ground can reduce the coupling between the human body and the antenna, and it also brings the convenience of integration with clothes. The proposed antenna is fabricated and measured on pork, and the impedance bandwidth of 63 MHz for on-body mode and 303 MHz for off-body mode is achieved. Besides, the bending characteristics and the specific absorption rate (SAR) are also analyzed, which meet the requirement. These characteristics make the proposed antenna a good choice for WBAN dual-mode applications.

1. INTRODUCTION

With the progress of electronic technology, wearable and implantable devices will be widely used. These devices transmit data through wireless body area network (WBAN). It is usually considered as three occasions, in-body, on-body, off-body, corresponding to the communications between the device on the body and the implantable device, the device on the human body, and the external node, respectively [1]. This requires that the antennas in these devices have different radiation patterns for different modes on the human body, with an omnidirectional radiation pattern for on-body mode and a broadside radiation pattern for in- and off-body modes [2]. Meanwhile, the polarization of the antenna also needs to be considered for different modes. The propagation loss of vertical polarization (VP) waves along the body surface is lower than that of horizontal polarization (HP) waves for on-body mode [3]. For in- and off-body modes, the introduction of circular polarization (CP) can reduce the loss caused by polarization mismatch between linearly polarized antennas (LP) [4].

Recently, dual-mode wearable antenna has gained a lot of attention, because it can bring more communication links than a single-mode antenna, thus expanding the function of wearable devices. There have been many studies to implement two radiation patterns, such as exciting two patches through two ports [5, 6], utilizing dual-band operation to generate different modes [7, 8], and reconfigurable design [9, 10]. These published papers are based on a rigid substrate, which has good robustness, but it often brings discomfort to the human body due to its large size. By contrast, the textile substrate can be better embedded in clothing without discomfort for its bendable property [11]. In [12], the combination of a microstrip ring and a meandered microstrip patch antenna realizes single band dual-mode radiation by the use of textiles. In [13], a dual-band and dual-mode antenna is realized on polydimethylsiloxane (PDMS). A radiation pattern reconfigurable antenna based on felt is proposed in [14]. However, it should be noted that the effect of textile bending on antenna performance cannot be ignored. Therefore, a

Received 29 March 2020, Accepted 2 June 2020, Scheduled 8 June 2020
* Corresponding author: Shaojun Fang (fangshj@dlmu.edu.cn).
The authors are with the School of Information Science and Technology, Dalian Maritime University, Dalian, Liaoning 116026, China.

design with good robustness and comfort is an important requirement for a wearable antenna. The movement of the human body will bring a challenge to radiofrequency link quality for wearable devices, so a CP antenna is chosen for its strong anti-interference ability [4]. Although there have been many studies on CP wearable antennas [15–17], few of them have introduced CP radiation to dual-mode antennas.

In this work, a compact dual-band and dual-polarized antenna integrated into textile is presented. An omnidirectional pattern of vertical polarization and a broadside pattern of CP are realized at 2.45 GHz and 5.8 GHz, respectively. Both radiation patterns at the two bands are realized on the same patch through the tuning of slots and pins, which bring a simple structure. The combination of a compact rigid substrate and a flexible felt makes the antenna have good robustness and comfort to the human body, and also reduces the coupling between the antenna and the human body. The antenna is fabricated and measured, and its performance is simulated on the human body tissue and measured on pork, respectively. Besides, the bending characteristics of textile materials are also analyzed. The specific absorption rate (SAR) is simulated, which meets the requirement of the IEEE C95.3 standard.

2. ANTENNA DESIGN

Figure 1 shows the structure of the proposed antenna. On a basic circular patch antenna, center-feed is adopted, and two annular slots are introduced to realize CP, which has been proposed in [18]. Two mutually perpendicular tabs of the outer annular slot will produce two mutually perpendicular linear polarizations. By adjusting the angle deviation between the tab of the inner annular slot and the two tabs of the outer annular slot, a 90° phase shift between the two linear polarizations can be produced, to realize the circularly polarized radiation. Fig. 2(a) shows the electric field distribution of the patch surface at different phases of 5.8 GHz, and it shows a left-handed CP (LHCP) radiation. A good impedance matching can be achieved by optimizing the size of the inner circular patch and the two annular slots.

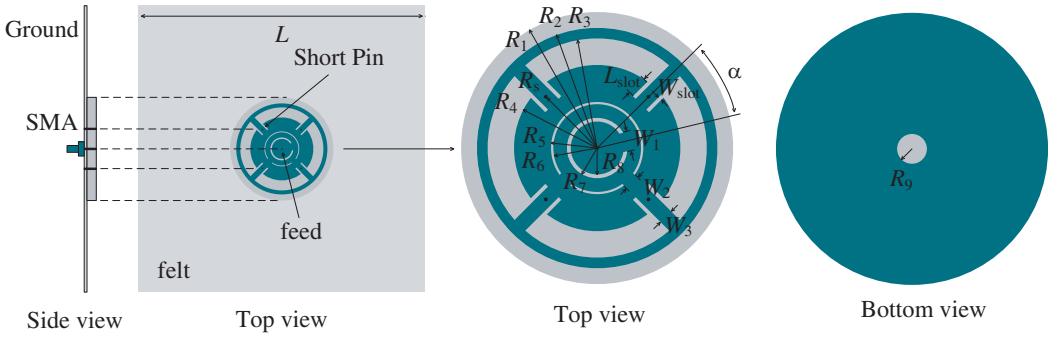

Figure 1. Antenna geometry. (a) Substrate with felt. (b) Two sides of the substrate.

Another outer circular ring patch is connected to the inner circular patch by four branches. The omnidirectional radiation pattern of TM_{01} is excited at 2.45 GHz by the introduction of four short pins [19]. The electric field distribution can be observed in Fig. 2(b). But at this time, the large input impedance of the antenna makes it difficult to match. To solve this problem, a felt with an all ground is integrated with the antenna, which makes the original ground at the bottom of the rigid substrate a parasitic patch. Due to the capacitive coupling between the parasitic patch and the top patch, the input impedance and quality factor Q are reduced, which brings a good impedance matching and a wider bandwidth [20]. As shown in Fig. 3, the real part of the input impedance has decreased a lot, and the S_{11} has become satisfactory. The resonance frequency is also slightly reduced because of the increase of capacitance.

The rigid substrate is fixed to the felt by the four short pins. Two slots are cut along the branch of the outer ring patch and inner circular patch at all the four branches, which can reduce resonance

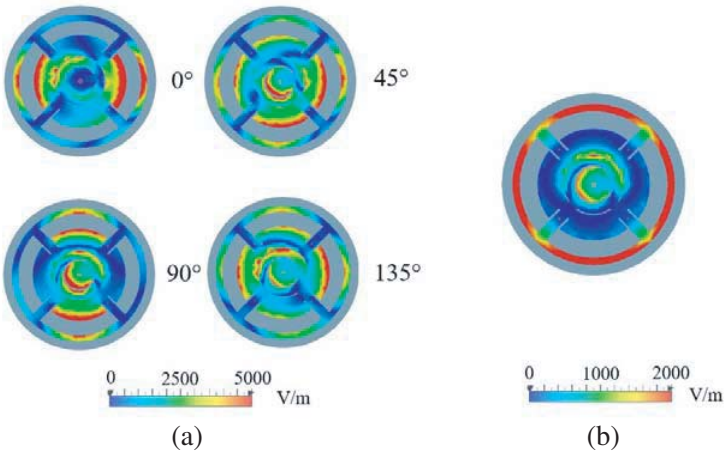

Figure 2. Electric field distributions on the patch at (a) 5.8 GHz of different phases, (b) 2.45 GHz.

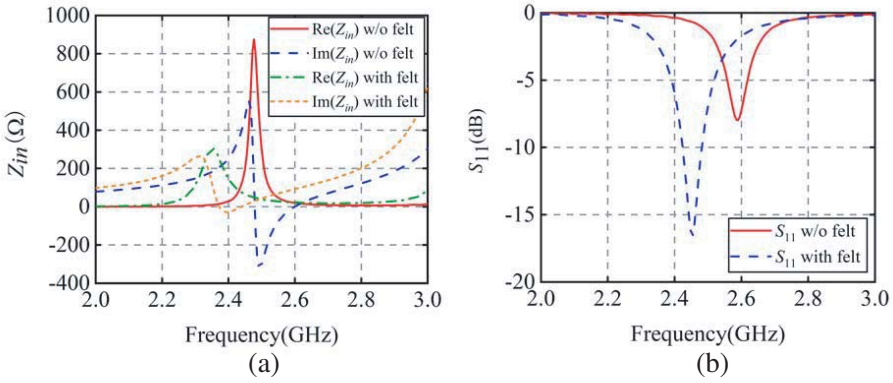

Figure 3. The influence of felt at the lower band on (a) Z_{in}, (b) S_{11}.

frequency by extending the current path of the upper band to miniaturize the inner patch [21]. Finally, the geometry of the antenna is simulated and optimized by CST Microwave Studio, and the specific dimensions are shown in Table 1.

Table 1. Dimensions of the design (Unit: mm, except α).

R_1	18	R_7	4	W_3	2
R_2	15.9	R_8	3.5	W_{slot}	0.5
R_3	14.5	R_9	2	L_{slot}	2.8
R_4	11	R_s	9.6	L	100
R_5	6.1	W_1	2.5	α	35°
R_6	5.8	W_2	2		

3. FABRICATION AND RESULTS

Photographs of the fabricated antenna are shown in Fig. 4, and it is composed of a rigid substrate named F4B ($\varepsilon_r = 2.65$, $\tan\delta = 0.003$) with a thickness of 3.2 mm and a 1-mm-thick felt ($\varepsilon_r = 1.2$, $\tan\delta = 0.02$). The 0.2-mm-thick conductive fabric with a conductivity of 1.2×10^5 S/m is chosen as the ground plane.

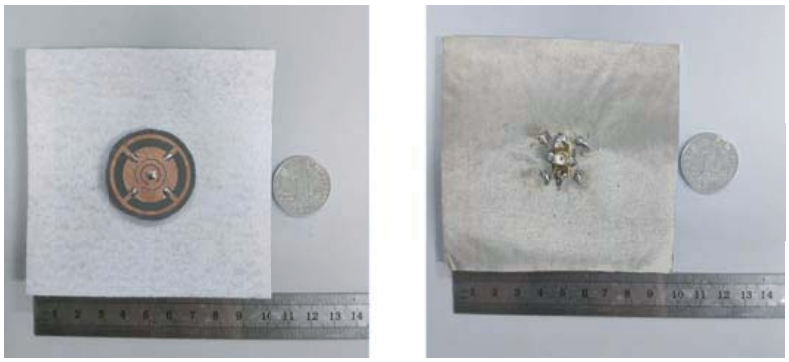

(a) (b)

Figure 4. The fabricated prototype. (a) Top view. (b) Back view.

(a) (b) (c)

Figure 5. Experiment setup on body. (a) Simulated on body tissue. (b) Measured S_{11} on pork. (c) Measured radiation pattern on pork.

Table 2. Electrical properties and thicknesses of the human body tissue.

Tissue	2.45 GHz		5.8 GHz		Thickness (mm)
	ε_r	σ (S/m)	ε_r	σ (S/m)	
Skin	37.50	1.49	35.10	3.71	1.5
Fat	5.28	0.10	4.95	0.29	10.0
Muscle	52.67	1.77	48.48	4.96	20.0

Then the antenna is simulated and measured in free space (FS). A three-layer body tissue model of 300 mm × 300 mm is established to carry out the simulation to verify the antenna performance on the human body, shown as in Fig. 5(a). The model consists of muscle, fat, and skin, whose characteristics are shown in Table 2 [1]. There is a height of 5 mm between the antenna and human tissue. In the measurement setup on body (OB), pork is used instead of the human body for safety, shown in Figs. 5(b), (c). For the convenience of measurement, a small right angle bent connector is used to connect the antenna and coaxial line. When measuring the radiation patterns in an anechoic chamber, two foams are placed between felt and pork, which can play a fixed role.

The simulated and measured results of S_{11} of the antenna are shown in Fig. 6. As can be seen, the measured results shift slightly. This may be caused by two main reasons, including the deviation of the relative permittivity of the rigid substrate and the tolerances of fabrication. In free space, the measured −10 dB impedance bandwidth at the lower band is 67 MHz (∼ 2.73%) and at the up band is 282 MHz (∼ 4.86%), while 3-dB axial ratio (AR) bandwidth is 78 MHz (∼ 1.34%). When the antenna is placed

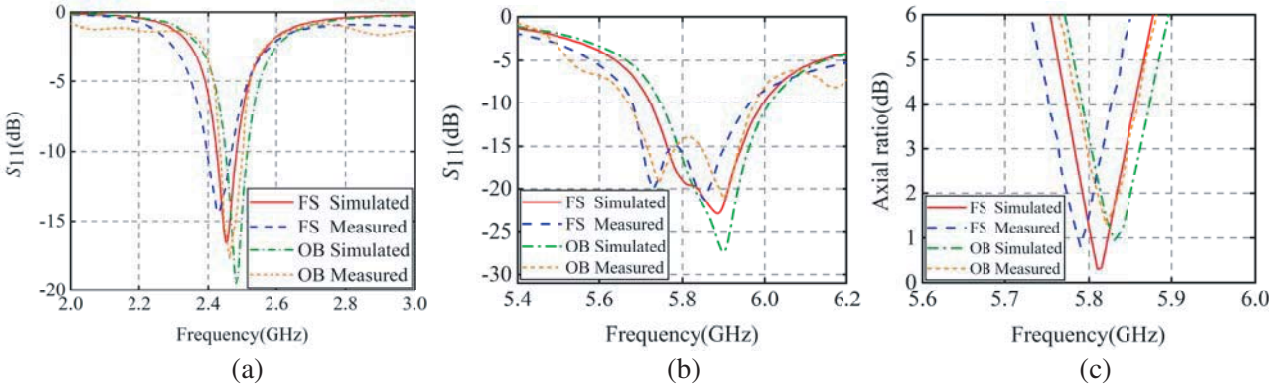

Figure 6. Results in free space and on body. (a) S_{11} at the lower band. (b) S_{11} at the up band. (c) AR at the up band.

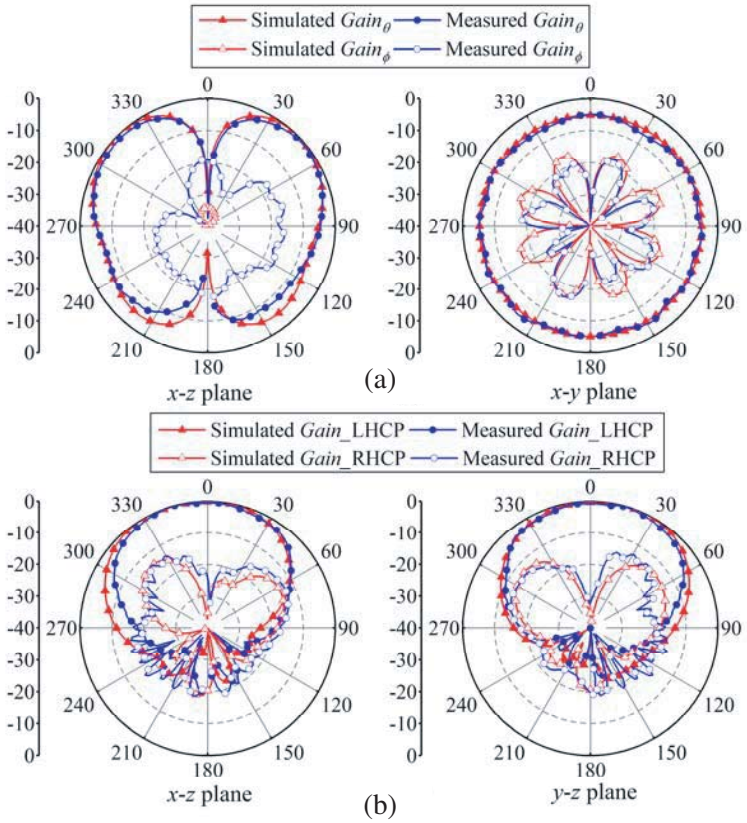

Figure 7. Radiation patterns in free space (a) On-body mode. (b) Off-body mode.

on the pork, the measured bandwidths of the two bands are 63 MHz ($\sim$ 2.57%) and 303 MHz ($\sim$ 5.22%), respectively, while 3 dB AR bandwidth is 50 MHz ($\sim$ 0.86%). The simulated and measured radiation patterns in the free space of the proposed antenna are shown in Fig. 7. At 2.45 GHz, an omnidirectional pattern with a measured peak gain of 2.5 dBi is observed. At 5.8 GHz, a broadside pattern with a measured peak gain of 5.9 dBi can be seen. Fig. 8 shows the results measured on pork, with a gain of 1.9 dBi at 2.46 GHz and 5.0 dBi at 5.82 GHz. Due to the absorption of energy by the human body, the gain of the antenna is slightly reduced. The measured results of radiation patterns agree well with the simulated ones, but there are some deviations. On the one hand, it is caused by the difference in the

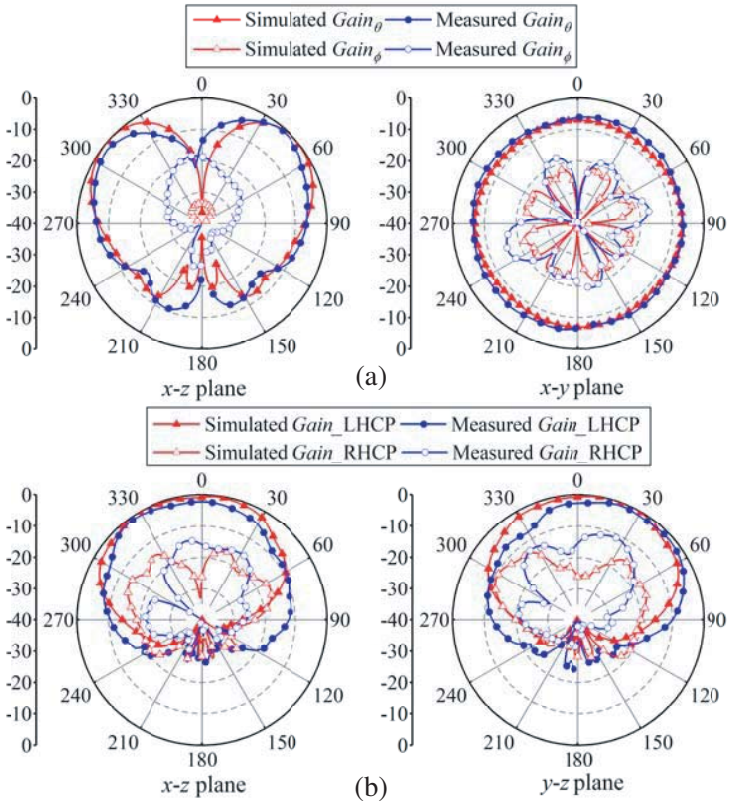

Figure 8. Radiation patterns on pork (a) On-body mode. (b) Off-body mode.

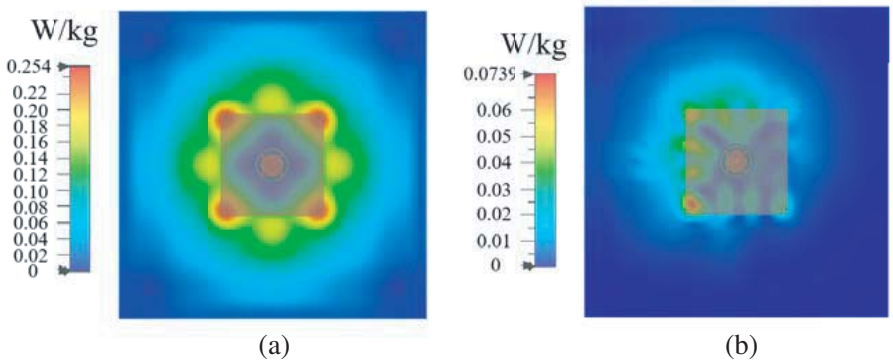

Figure 9. Simulated SAR distribution on body tissue mode at (a) 2.46 GHz, (b) 5.82 GHz.

relative permittivity between the human body model and pork. On the other hand, the deformation caused by fixing the antenna on the pork will also affect the test results of the radiation pattern.

To ensure the safety of human body exposed to electromagnetic radiation, the simulation of SAR is carried out on the human tissue model shown in Fig. 9, which shows that the maximum SAR value at 2.46 GHz is 0.254 W/kg, while at 5.82 GHz it is 0.074 W/kg, both of which are less than the standard of 1.6 W/kg over 1-g tissue in IEEE C95.3 [22]. Due to the unevenness of the human body, the antenna will also bend when it is worn on the human body. To verify its performance, the felt is bent with different radius of R. The simulation results are shown in Fig. 10. With the decrease of the bending radius, S_{11} slightly deviates at 2.45 GHz, and the impedance matching becomes worse. When $R = 20$ mm, this bending radius hardly occurs on the human body, but its performance is acceptable. At 5.8 GHz, the performance is almost unaffected no matter how small the bending radius is, which shows the robustness.

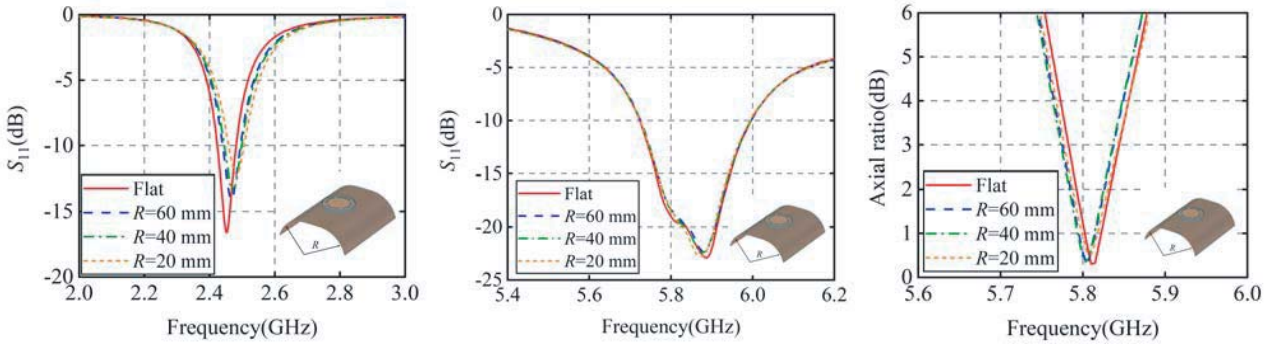

Figure 10. Results with different R. (a) S_{11} at the lower band. (b) S_{11} at the up band. (c) AR at the up band.

Besides, this work is compared with some current researches in Table 3. It can be observed that the footprint of this work is the smallest over these designs, which will bring a good human comfort. Most of the previous studies on dual-mode antennas only focus on line polarization, but this design of introducing circularly-polarized radiation for off-body mode can enhance the anti-interference of the link. These advantages make the proposed antenna a better choice in the application of WBAN.

Table 3. Comparison with published references.

Ref. No	Footprint (mm^2)*	f_0 (GHz)	Pattren#	Polarisation	BW (MHz)
[5]	$30 \times 30 \times \pi$	2.4/5.8	O/B	LP/LP	105/100
[6]	$34 \times 34 \times \pi$	2.45/2.45	O/B	LP/LP	80/180
[7]	$24 \times 24 \times \pi$	2.45/5.8	O/B	LP/LP	26/131
[8]	$24 \times 24 \times \pi$	2.45/2.45	O/B	LP/LP	83/25
[9]	30×45	2.45/5.8	B/O	LP/LP	120/16
[10]	44×44	2.45/5.8	O/B	LP/LP	103/870
This work	$\mathbf{18 \times 18 \times \pi}$	**2.45/5.8**	**O/B**	**LP/CP**	**63/303**

* Only considering the rigid substrate, except textile.
\# O: Omnidirectional, B: Broadside.

4. CONCLUSION

In the letter, a dual-band and dual-polarized antenna integrated into textile for WBAN dual-mode applications is proposed. A vertically polarized omnidirectional radiation pattern is generated at 2.45 GHz for on-body mode, while a circularly polarized (CP) broadside radiation pattern resonates at 5.8 GHz for off-body mode. The operation of dual-band, dual-mode, and dual-polarized can be realized on a small substrate only by using the loading of slots and pins, which makes the antenna have a compact and simple structure. Meanwhile, a large ground is introduced with the textile, which reduces the mutual coupling between the antenna and the human body. The impedance bandwidth measured at the lower band is 63 MHz, and at the upper band it is 303 MHz with 3-dB AR bandwidth being 50 MHz. The peak gains are 1.9 dBi at 2.46 GHz and 5.0 dBi at 5.82 GHz, respectively, when being measured on pork. In the case of bending, the antenna can also maintain good performance. The simulation of the SAR is carried out, which meets the requirement of the IEEE C95.3 standard. Compared with the previous studies, the proposed antenna introduces circularly-polarized radiation for the off-body mode to enhance the anti-interference of the link. Meanwhile, its size is smaller, while ensuring comfort and robustness. These characteristics make the proposed antenna valuable for WBAN dual-mode applications.

REFERENCES

1. Hall, P. S. and Y. Hao, *Antennas and Propagation for Body-centric Wireless Communications*, Artech House Publishers, Boston, 2006.
2. Conway, G. A. and W. G. Scanlon, "Antennas for over-body-surface communication at 2.45 GHz," *IEEE Trans. Antennas and Propag.*, Vol. 57, No. 4, 844–855, Apr. 2009.
3. Dumanli, S., "On-body antenna with reconfigurable radiation pattern," *2014 IEEE MTT-S International Microwave Workshop Series on RF and Wireless Technologies for Biomedical and Healthcare Applications (IMWS-Bio2014)*, 1–3, London, UK, Dec. 2014.
4. Li, K., L. Li, Y. Cai, C. Zhu, and C. Liang, "A novel design of low-profile dual-band circularly polarized antenna with meta-surface," *IEEE Antennas Wirel. Propag. Lett.*, Vol. 14, 1650–1653, 2015.
5. Liu, Z. and Y. Guo, "Compact low-profile dual band metamaterial antenna for body centric communications," *IEEE Antennas Wirel. Propag. Lett.*, Vol. 14, 863–866, 2015.
6. Masood, R., C. Person, and R. Sauleau, "A dual-mode, dual-port pattern diversity antenna for 2.45-GHz WBAN," *IEEE Antennas Wirel. Propag. Lett.*, Vol. 16, 1064–1067, 2017.
7. Tak, J., S. Woo, J. Kwon, and J. Choi, "Dual-band dual-mode patch antenna for on-/off-body WBAN communications," *IEEE Antennas Wirel. Propag. Lett.*, Vol. 15, 348–351, 2016.
8. Zhao, C. and W. Geyi, "Design of a dual band dual mode antenna for on/off body communications," *Microw. Opt. Technol. Lett.*, Vol. 62, No. 1, 514–520, 2020.
9. Tong, X., C. Liu, and X. Liu, "Dual-band on-/off-body reconfigurable antenna for wireless body area network (WBAN) applications," *Microw. Opt. Technol. Lett.*, Vol. 60, No. 4, 945–951, 2018.
10. Tong, X., C. Liu, X. Liu, H. Guo, and X. Yang, "Switchable on-/off-body antenna for 2.45 GHz WBAN applications," *IEEE Trans. Antennas and Propag.*, Vol. 66, No. 2, 967–971, Feb. 2018.
11. Bhattacharjee, S., S. Maity, S. R. B. Chaudhuri, and M. Mitra, "A compact dual-band dual-polarized omnidirectional antenna for on-body applications," *IEEE Trans. Antennas and Propag.*, Vol. 67, No. 8, 5044–5053, Aug. 2019.
12. Mendes, C. and C. Peixeiro, "A dual-mode single-band wearable microstrip antenna for body area networks," *IEEE Antennas Wirel. Propag. Lett.*, Vol. 16, 3055–3058, 2017.
13. Simorangkir, R. B., Y. Yang, and L. Matekovits, "Dual-band dualmode textile antenna on PDMS substrate for body-centric communications," *IEEE Antennas Wirel. Propag. Lett.*, Vol. 16, 677–680, 2017.
14. Yan, S. and G. A. E. Vandenbosch, "Radiation pattern-reconfigurable wearable antenna based on metamaterial structure," *IEEE Antennas Wirel. Propag. Lett.*, Vol. 15, 1715–1718, 2016.
15. Chen, S. J., T. Kaufmann, D. C. Ranasinghe, and C. Fumeaux, "A modular textile antenna design using snap-on buttons for wearable applications," *IEEE Trans. Antennas and Propag.*, Vol. 64, No. 3, 894–903, Mar. 2016.
16. Ullah, U., I. B. Mabrouk, and S. Koziel, "A compact circularly polarized antenna with directional pattern for wearable off-body communications," *IEEE Antennas Wirel. Propag. Lett.*, Vol. 18, No. 12, 2523–2527, Dec. 2019.
17. Hu, X., S. Yan, and G. A. E. Vandenbosch, "Compact circularly polarized wearable button antenna with broadside pattern for U-NII worldwide band applications," *IEEE Trans. Antennas and Propag.*, Vol. 67, No. 2, 1341–1345, Feb. 2019.
18. Zheng, K. and Q. Chu, "A novel annular slotted center-fed beidou antenna with a stable phase center," *IEEE Antennas Wirel. Propag. Lett.*, Vol. 17, No. 3, 364–367, Mar. 2018.
19. Hou, Q., H. Tang, Y. Liu, and X. Zhao, "Dual-frequency and broadband circular patch antennas with a monopole-type pattern based on epsilon-negative transmission line," *IEEE Antennas Wirel. Propag. Lett.*, Vol. 11, 442–445, 2012.
20. Al-Zoubi, A., F. Yang, and A. Kishk, "A broadband center-fed circular patch-ring antenna with a monopole like radiation pattern," *IEEE Trans. Antennas and Propag.*, Vol. 57, No. 3, 789–792, Mar. 2009.

21. Yang, F. and X. X. Zhang, "Slitted small microstrip antenna," *Proc. IEEE Antennas Propagation Symp.*, Vol. 2, 1236–1239, Atlanta, GA, USA, 1998.
22. "IEEE recommended practice for measurements and computations of radio frequency electromagnetic fields with respect to human exposure to such fields, 100 kHz to 300 GHz," *IEEE Standard C95.3-2002*, i–126, 2002.